

Self-organized criticality in the Bean state in $YBa_2Cu_3O_{7-x}$ thin films.

C. M. Aegerter, M. S. Welling, and R. J. Wijngaarden

Division of Physics and Astronomy, Faculty of Sciences, Vrije Universiteit, De Boelelaan 1081, 1081HV Amsterdam, The Netherlands

(April 14, 2024)

The penetration of magnetic flux into a thin film of $YBa_2Cu_3O_{7-x}$ is studied when the external field is ramped slowly. In this case the flux penetrates in bursts or avalanches. The size of these avalanches is distributed according to a power law with an exponent of $\alpha = 1.29(2)$. The additional observation of finite-size scaling of the avalanche distributions, with an avalanche dimension $D = 1.89(3)$, gives strong indications towards self-organized criticality in this system. Furthermore we determine exponents governing the roughening dynamics of the flux surface using some universal scaling relations. These exponents are compared to those obtained from a standard roughening analysis.

PACS numbers: 05.65.+b, 74.72.Bk, 64.60.Ht, 74.25.Qt

The critical state in a type-II superconductor shows a powerful analogy to a granular pile, which was already noted by de Gennes in the 1960s [1]. With the advent of self-organized criticality (SOC) [2], the avalanche behavior of granular piles was intensely studied [3]. This is because SOC was thought of as a general mechanism to explain the intermittent behavior of slowly driven systems far from thermodynamic equilibrium. The experimental verification of SOC, however, was not straightforward. Power-law distribution of avalanches was not observed in many experiments [4]. One of the hallmarks of critical behavior, finite-size scaling, was only found in a few cases, most notably in experiments on a one-dimensional (1d) pile of rice [5], as well as in a 1d pile of steel balls with a random distribution of balls in the bottom layer [6]. The only study of finite size scaling in a 2d system to date, is to our knowledge a study by some of us on the properties of a 2d pile of rice [7], which is qualitatively similar to the one presented here.

Given the classical analogy with granular piles [8], the critical state in superconductors was also quickly proposed as a SOC system [9]. Experimentally, magnetic vortices are well suited to study SOC, since kinetic effects, which can lead to deviations from critical behavior in sand-piles [5,10], are naturally suppressed due to their overdamped dynamics [11]. Just as in the case of granular piles, however, the experimental confirmation of this conjecture has been controversial. While power-law behavior in the avalanche distribution has been observed by most authors [12,13], finite-size scaling was not observed so far in the case of the critical state in superconductors. This is because most of the studies [12,14], were carried out using magnetization measurements, which only give information on the overall behavior of the whole of the sample. This corresponds to only considering edge avalanches in a sand-pile, which do not capture the full dynamics and may therefore give a biased picture [10]. More recent investigations using arrays of miniature Hall-probes [13], do give insights into internal avalanches and the complete dynamics, but only give information from

a few selected points in the sample, which makes testing for finite-size scaling impossible.

In this letter, we study the local changes in the magnetic flux over the whole central area of a sample. This is done via a highly sensitive magneto-optic setup, which can resolve flux densities of 0.2 mT over an area of $5 \times 5 \mu\text{m}^2$. This implies that flux changes corresponding to $2.5 \phi_0$ can be resolved, where $\phi_0 = h/2e$, is the magnetic flux quantum (the flux of a single vortex). Furthermore, since we observe a large field of view, different size subsets can be studied leading to the possibility of observing finite-size scaling. Given the finite-size scaling exponents, one can determine the roughening and dynamical exponents of the flux-surface from universal scaling relations. Comparing these results with those determined directly from the surface properties [15], gives good agreement. Furthermore, the exponents fulfill the scaling relation $\alpha + z = 2$, valid for the well known driven interface model given by the Kardar-Parisi-Zhang (KPZ) equation [16] (see below).

The experiments were carried out on a thin film of $YBa_2Cu_3O_{7-x}$ (YBCO), grown on a $NdGaO_3$ substrate to a thickness of 80 nm using pulsed laser ablation [17]. The pinning sites in the sample are uniformly distributed and consist mostly of screw dislocations acting as point pins [18]. A polarization microscope was placed in an Oxford Instruments cryomagnets capable of a maximum field of 1 T and cooling to a temperature of 1.8 K. The sample was cooled in zero field to 4.2 K, at which point the external field was slowly increased in steps of $\mu_0 H = 50$ T, after which the sample was allowed to relax for 10 s before an image was taken. In a magneto-optical experiment, the flux density $B_z(x,y)$ at the surface of the sample is measured via an indicator layer showing a strong Faraday effect. The polarization of the incoming light is turned in proportion to the flux density in the indicator layer. A cross-polarized analyzer will thus admit light from regions with non-zero magnetic flux density [19]. However, in order to determine the rotation angle (and thus the flux density B_z) directly, including its sign, we employ

a recently developed magneto-optic image lock-in amplifier [20], using a modulation of the incoming polarization vector. The output of the instrument gives directly the Faraday angle for each pixel, independent of spatial inhomogeneities in the illumination.

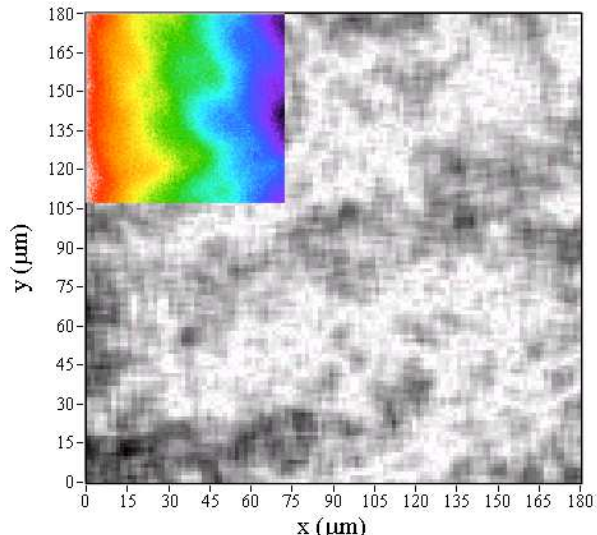


FIG. 1. Snapshot of a flux-avalanche. Shown is the difference between two consecutive field-profiles $B(x,y)$. The scale goes from 0 (white) to 0.4 mT (black). The area-integral over this difference corresponds to the size of the flux-jump. In order to determine the roughness exponent of the whole surface, we also need to determine the fractal dimension of the active sites in such an avalanche (see text). The inset shows the flux distribution $B_z(x,y)$ in the same part of the sample. Here the scale varies from 0 mT (black) to 12 mT (white). Lines of constant field can be identified by the different shades.

The data analyzed here come from a series of nine experimental runs, each consisting of 300 time-steps. Of these steps only the last 140 in each run were used, in order to have a critical state established in the whole region of the sample used for analysis. The size and shape of the avalanches was determined from the difference $B_z(x,y)$ of two consecutive images (see Fig. 1). From this difference, the average increase in the applied magnetic field, due to the step-wise field-sweep, was subtracted in order to solely study the avalanches. The external fields were determined from a region well outside the sample, which was also in the field of view. Once the incremental field difference is determined, the size of an avalanche, corresponding to the displaced amount of flux, is obtained from $\Delta\Phi$ via integration over the whole area

$$s = \frac{1}{2} \int \int B(x,y) dx dy \quad (1)$$

The average increase in the external field is in good agreement with the increase in flux density of 50 T between images. The resulting time series of the avalanche behavior of all the experiments is shown in Fig. 2. In this figure, $\Delta\Phi$ was integrated over the whole area of 180x180

μm^2 in each time step. As can be seen, the evolution of the magnetic flux inside the sample is intermittent with occasional large jumps.

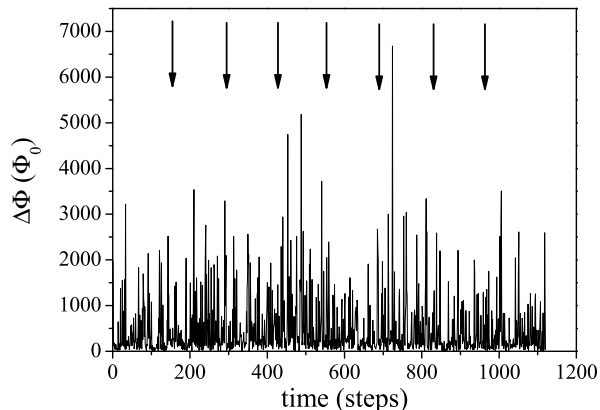


FIG. 2. The time evolution of the magnetic flux inside the sample over all nine experiments. The magnetic field-difference $\Delta\Phi$ has been integrated over the whole surface of $180 \times 180 \mu\text{m}^2$ and the average flux increase has been subtracted. The evolution takes place in the form of flux jumps or avalanches of various sizes, which are summarized in the histogram of Fig. 3. The different experimental runs are separated by arrows.

In order to check the data for finite size scaling, we also integrated $\Delta\Phi$ over subsets of the image of a linear size of $L = 90, 45$ and $15 \mu\text{m}$ respectively. The histograms of the avalanche size distribution for these data-sets are shown unscaled in Fig. 3a. As can be seen, the smallest avalanches correspond to a flux change of 2-3 Φ_0 , corresponding to the resolution of the measurement. Taking all of the data together we observe a power-law distribution over more than three decades. The slope of the black line gives the exponent of the distribution, $\alpha = 1.30(5)$. In Fig. 3b we show the same data, but now the probabilities are scaled with s^{α} and the avalanche sizes are scaled with L^D . As can be seen, there is very good curve collapse indicating the presence of finite size scaling [21]. This means that the avalanche size distribution function is given by

$$P(s;L) = s^{-\alpha} f\left(\frac{s}{L^D}\right); \quad (2)$$

where $f(x)$ is constant up to a cutoff scale s_0 / L^D . The values of the exponents used to obtain curve collapse are $\alpha = 1.29(2)$ and $D = 1.89(3)$. Note that here, we have carried out the finite size scaling by way of subdividing the whole image rather than carrying out experiments with different size samples. We have checked by means of simulations of the 2d Oslo-model that such a subdivision into finite-size samples leads to the same scaling exponents as a curve collapse of different simulations of finite size. Furthermore, an independent measurement of D , directly using a box counting method [22] in 3d yields

$D = 1.92(5)$, consistent with the value from finite size scaling.

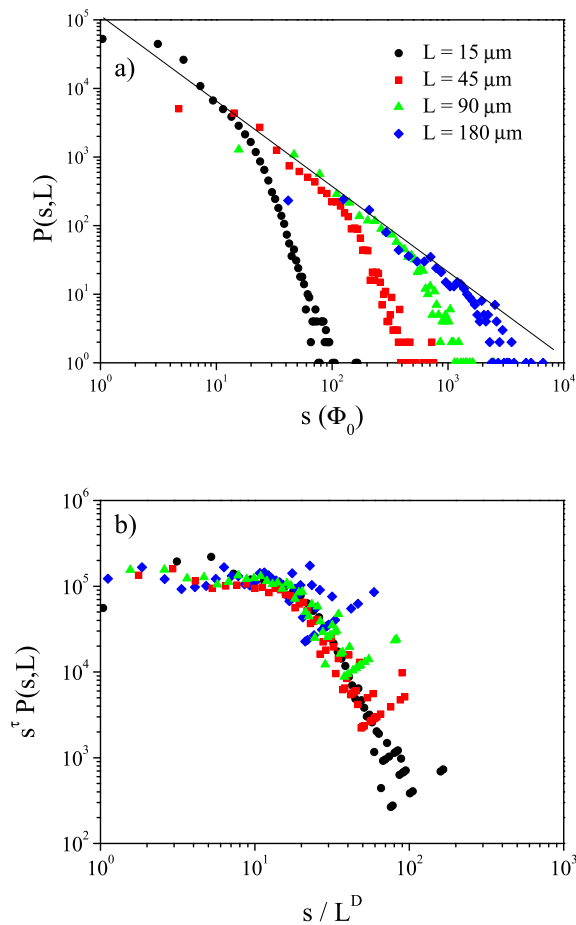


FIG. 3. (a) The direct avalanche size distribution for different sizes of windows (180, 90, 45, and 15 μm respectively). There is an envelope to the distribution in the form of a power-law indicated by the black line over more than three decades with an exponent of $\tau = 1.30(5)$. (b) The scaled size distributions showing a curve collapse. The exponents used in the finite-size scaling are $\tau = 1.29(2)$ and $D = 1.89(3)$.

It has already been noted [23] that the front of penetrating flux shows kinetic roughening. Similarly, the surface $B_z(x; y)$ in two dimensions can be shown to be self-affine, with a roughness exponent α , characterizing the growth of the interface width w_{sat} with the system size, w_{sat}/L and a dynamic exponent z characterizing the saturation time of the width. In such an analysis of the present data, discussed elsewhere [15], the roughness exponent was found to be $\alpha = 0.73(5)$ and the dynamic exponent was found to be $z = 1.38(10)$. Using the universal scaling relations derived by Paczuski et al. [24] for various SOC models, these exponents characterizing the roughness and growth of the surface can also be determined from the scaling exponents of the avalanche distribution. This indicates the fact that the roughening of the surface originates from the avalanche distribution

and its underlying dynamics.

Let us first discuss the roughness exponent. According to the finite size scaling, an avalanche of the cut-off size will scale like s_{co}/L^D . Similarly, the size of such an avalanche will roughly be given by $s_{\text{co}} \sim w_{\text{sat}} L^{d_B}$, where d_B is the fractal dimension of the area of an avalanche. Equating the two expressions for s_{co} , one obtains $w_{\text{sat}}/L^D \sim L^{d_B}$ and hence

$$\alpha = D - d_B; \quad (3)$$

in agreement with Ref. [24]. In order to determine the roughness exponent from the avalanches, we therefore have to measure the fractal dimension, d_B , of the avalanches area, which was done using a simple box-counting method [22]. To this end, avalanches which were one standard deviation bigger than average were binarized, yielding a distribution of active clusters used in the determination of the fractal dimension. The result for one such cluster can be seen in Fig. 4, where the number of active pixels of the avalanche is shown as a function of the length scale. Averaged over all clusters analyzed, the fractal dimension, given by the slope of the line in Fig. 4, is $d_B = 1.18(5)$. From this we determine the roughness exponent as $\alpha = 0.71(5)$, in good agreement with that determined from a roughness analysis (via the correlation function and the power-spectrum) of the surface fluctuations [15].

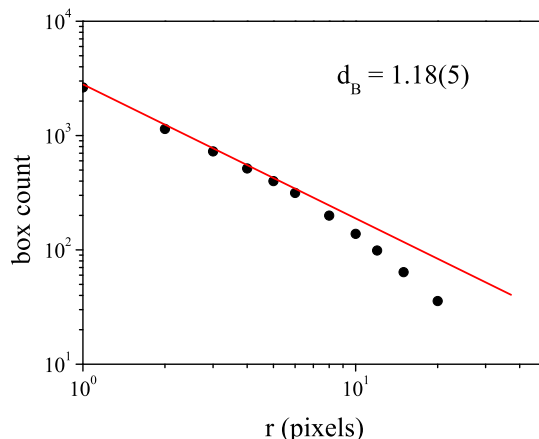


FIG. 4. Determination of the fractal dimension of the active clusters in an avalanche using the box counting method. In this determination, avalanches more than one standard deviation larger than the average size have been studied. The analysis of one such cluster is shown. The fractal dimension is given by the slope of the straight line. Averaged over all clusters, this leads to a fractal dimension of the active clusters of $d_B = 1.18(5)$.

The dynamic exponent, z , can be obtained from a similar argument. The scaling of the crossover-time with the system size is described by z , t_c/L^z . This crossover-time can be roughly estimated from the time it takes for an avalanche of the cut-off size s_{co} to appear. Since flux is added to the system in constant steps, Φ_0 , the number

of vortices added until a cut-off avalanche occurs is given by t_c . On the other hand, the flux added will also be removed in smaller avalanches. The total flux necessary to be introduced in order to obtain an avalanche of size s_{co} can be estimated from integrating over all avalanche sizes up to the one of size s_{co} :

$$t_c / L^D \sim \int_0^{s_{co}} s^p(s) ds / s_{co}^2 \quad (4)$$

Using s_{co} / L^D , we obtain $t_c / L^D \sim (2 - z)$, which immediately leads to the scaling relation

$$z = D(2 - z) \quad (5)$$

Again, this is also in agreement with the universal scaling relation derived by Paczuski et al. [24]. Inserting the values determined above, we obtain $z = 1.34$ (4), again in good agreement with that determined via roughness analysis [15].

In conclusion, we have shown that the distribution of the size of flux jumps in an YBCO thin film is not only given by a power-law but also shows finite size scaling. Due to universal scaling relations valid for a SOC state [24], the exponents determined via finite-size scaling can also be used to describe other properties of the system. One such example is the roughening of the magnetic flux surface. Here the statistical properties of the self-affine structure are built up by the penetrating flux, such as the roughness and dynamical exponent can be derived from the structure and dynamics of the flux-avalanches using relations (3) and (5). These characteristic exponents can however also be determined directly, via a roughness analysis [15], the results of which can be compared to those obtained via the avalanche dynamics. As discussed above, we find excellent agreement between the exponents determined in these separate ways. The critical state observed in the YBCO thin films can be seen as a realization of a 2d roughening system, albeit with a self-organized dynamics. In this context, we note that the roughness and dynamical exponents fulfill the general KPZ scaling relation $\nu + z = 2$, which is an exact result also in 2d.

In the future, the magnetic flux structures in superconductors, as the ones studied here, may be used as an ideal experimental system with which to study non-equilibrium phenomena, especially those of granular matter. In fact we find strong qualitative correspondence of the behavior of the vortices with that of a pile of rice [7] in terms of SOC behavior. However, in addition to the granular system, the superconducting system studied here allows for the presence and control of quenched noise due to pinning sites, whose influence on the statistical properties can then be studied experimentally as well. Moreover, the physics of the microscopic behavior of vortices is well studied [11], such that collective effects can be studied directly.

We would like to thank Jan Rector for the growth of the samples. This work was supported by FOM (Stichting voor Fundamenteel Onderzoek der Materie), which is

financially supported by NWO (Nederlandse Organisatie voor Wetenschappelijk Onderzoek).

-
- [1] P. G. deGennes Superconductivity of metals and alloys (Addison-Wesley, 1966).
 - [2] P. Bak, C. Tang, and K. Wiesenfeld, Phys. Rev. Lett. 59, 381 (1987) and Phys. Rev. A 38, 364 (1988).
 - [3] see e.g. H. M. Jaeger, C.-H. Liu, and S. R. Nagel, Phys. Rev. Lett. 62, 40 (1989); J. Rosendahl, M. Vekic, and J. E. Rutledge, Phys. Rev. Lett., 73, 537 (1994); or for a summary J. Feder, Fractals 3, 431 (1995).
 - [4] H. M. Jaeger, S. R. Nagel, and R. P. Behringer, Rev. Mod. Phys. 68, 1259 (1996); S. R. Nagel, ibid. 64, 321 (1992) and references therein.
 - [5] V. Frette et al., Nature (London) 379, 49 (1996).
 - [6] E. A. Itshuler et al., Phys. Rev. Lett. 86, 5490 (2001).
 - [7] C. M. Aegerter, R. Gunther, and R. J. Wijnngaarden, accepted for publication PRE (2003).
 - [8] A. M. Campbell, and J. E. Evetts, Adv. Phys. 21, 199 (1972); reprinted ibid 50, 1249 (2001); E. A. Itshuler, in Some contemporary problems of condensed matter physics in contemporary fundamental physics, V. V. Dvoeglazov, S. J. Vaev, and L. M. Gaggero (eds.), Nova Science Publishers (2001).
 - [9] C. Tang, Physica A 194 (1-4), 315 (1993); S. I. Zaitsev, Physica A 151, 411 (1992).
 - [10] J. Feder, Fractals (Plenum, New York, 1989).
 - [11] G. B. Latter et al., Rev. Mod. Phys. 66, 1125 (1995).
 - [12] S. Field, J. Witt, and F. Nori, Phys. Rev. Lett. 74, 1206 (1995); C. M. Aegerter, Phys. Rev. E 58, 1438 (1998).
 - [13] K. Behnia et al., Phys. Rev. B 61, R3815 (2000) and J. Mag. Mag. Mat. 226, 370 (2001).
 - [14] see e.g. R. J. Zieve et al., Phys. Rev. B 53, 11849 (1996); E. R. Nowak et al., Phys. Rev. B 55, 11702 (1997).
 - [15] M. S. Welling, C. M. Aegerter, and R. J. Wijnngaarden, to be published.
 - [16] M. Kardar, G. Parisi, and Y.-C. Zhang, Phys. Rev. Lett. 56, 889 (1986).
 - [17] B. Dam et al., Appl. Phys. Lett. 65, 1581 (1994).
 - [18] B. Dam et al., Nature 399, 439 (1999).
 - [19] R. P. Huebener Magnetic Flux Structures in Superconductors, (Springer, 2nd ed. 2000); M. R. Koblischka, and R. J. Wijnngaarden, Supercond. Sci. and Technol. 8, 199 (1995).
 - [20] R. J. Wijnngaarden et al., Rev. Sci. Instrum. 72, 2661 (2001).
 - [21] see e.g. A. L. Barabasi and H. E. Stanley Fractal Concepts in Surface Growth (Cambridge University Press, 1995).
 - [22] B. B. Mandelbrot, The fractal geometry of nature (Freeman, New York, 1983).
 - [23] R. Surdeanu et al., Phys. Rev. Lett. 83, 2054 (1999).
 - [24] M. Paczuski, S. Maslov, and P. Bak, Phys. Rev. E 53, 414 (1996); M. Paczuski, and S. Boettcher, Phys. Rev. Lett. 77, 111 (1996).